Frequency Synchronization Strategy for a PC-based DRM Receiver

Volker Fischer and Alexander Kurpiers
Institute for Communication Technology
Darmstadt University of Technology
Germany
{v.fischer, a.kurpiers}@nt.tu-darmstadt.de

***Abstract*— In this paper we propose a synchronization strategy for a PC-based DRM receiver. Given the parameters of the DRM system and the properties of off-the-shelf PC hardware, the requirements for the frequency synchronization are analyzed. Following these requirements an acquisition algorithm using the FFT and a tracking algorithm based on the incremental phase shift between two OFDM symbols is proposed. Both algorithms utilize the continuous frequency correction pilot tones in the DRM signal. Simulation results on different fading channels show that the synchronization scheme suits our needs.**

***Index Terms*— DRM, Digital Radio Mondiale, frequency synchronization**

I. Introduction

DIGITAL Radio Mondiale (DRM) is a new OFDM-based digital radio standard for the long-, medium- and short-wave ranges which was formed by an international consortium [1]. It is designed to use the same frequency allocation as the current analog systems to offer a high degree of compatibility. Even simulcast transmission is defined. The aim is to replace the analog system because the digital system has a lot of advantages. The audio quality is much better and additional digital information can be transmitted. Also, it is designed to cope perfectly with the strong channel impairments on the desired frequency bands. Long interleaving in combination with a multilevel channel code and various pilot cells make the signal robust against severe fading. Additionally, four different transmission modes (so called robustness modes A-D) are defined to adapt the system to different propagation conditions. These modes differ in guard-interval, symbol length and pilot structure.

The maximum bandwidth of a DRM signal is less than 20 kHz and the number of carriers is relatively small. These properties allow a real time software implementation of a DRM-receiver on a conventional personal computer (PC) using the sound card as input and output device. The system structure presented in this paper is optimized for this environment and all proposed algorithms are successfully verified on an existing realtime receiver implementation.

Since DRM uses OFDM modulation which is very sensitive to frequency offsets, frequency synchronization has an important influence on the performance of the receiver. To aid the frequency synchronization, the DRM standard defines three frequency pilots which are located at frequencies common for all system variants. These pilots are boosted in gain (two times the power of data cells) and the phases are chosen to ensure continuous tones. In this paper we use these pilots to perform a frequency synchronization which is sufficient for all DRM operation modes and channels.

The paper is structured as follows: Sect. II describes the effects of frequency and sample rate offset and evaluates the system requirements. The frequency tracking unit together with the sample rate offset estimator is described in Sect. III. In Sect. IV, the frequency acquisition algorithm is presented and simulation results are shown in Sect. V.

II. Requirements

A frequency offset between transmitter and receiver of an OFDM system has two effects on the demodulated signal. First, the demodulated data after the FFT unit is phase shifted and attenuated and second, the orthogonality of the OFDM symbols is destroyed causing inter-carrier-interference (ICI).

For small frequency offsets the output of the FFT unit for the l-th symbol and the k-th sub-carrier is given by [2]:

$$z_{l,k} = a_{l,k}\, e^{j2\pi\phi_k l \frac{N_s}{N}}\, \mathrm{sinc}(\phi_k) H_k + n_{\mathrm{ICI}_{l,k}} + \tilde{n}_{l,k}, \tag{1}$$

where N is the length of the FFT, N_s is the length of one OFDM symbol, H_k is the channel transfer function for sub-carrier k including time-invariant phase offsets due to frequency offsets, $n_{\mathrm{ICI}_{\mathrm{l,k}}}$ is the irreducible ICI noise caused by other sub-carriers $\neq k$ and $\tilde{n}_{l,k}$ is the white Gaussian noise with variance σ_n^2. The frequency error Δf and the sample rate offset $\zeta = \frac{T'-T}{T} = \frac{f_s - f_s'}{f_s'}$ are incorporated into the phase $\phi_k = \Delta f T_\mathrm{u} + \zeta k$, where T_u is the duration of the useful part of the OFDM symbol. The frequency error also causes an attenuation $\mathrm{sinc}(\phi_k)$ which is almost unity for small errors.

To judge which frequency offset is tolerable, a proven way is to look at the signal-to-noise ratio (SNR) loss caused by the additional ICI noise n_ICI. Speth and Meyr [2] give a limit to the frequency offset based on the tolerable SNR degradation $\Delta\gamma_\mathrm{max}$:

$$\Delta f\, T_\mathrm{u} < \frac{\sqrt{3}}{\pi}\sqrt{\frac{1}{\gamma}\left(1 - \frac{1}{\Delta\gamma_\mathrm{max}}\right)} \quad , \qquad (2)$$

where γ is the SNR. The maximum allowable frequency offset at a given SNR is plotted in Fig. 1. For

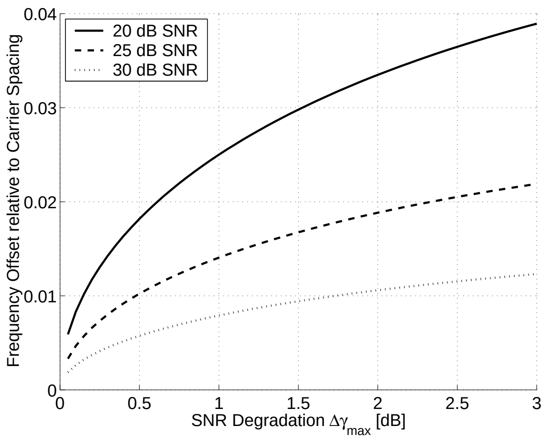

Fig. 1. Maximum allowable frequency offset $\Delta f\, T_\mathrm{u}$.

an SNR loss of less then 0.5 dB and a total SNR of 25 dB the allowable frequency offset $\Delta f\, T_\mathrm{u}$ should be less than 1 % of the carrier spacing.

In this paper we distinguish between two operation modes, the so called tracking mode and acquisition mode. First, in an acquisition step the initial frequency offset is estimated roughly so that as a second step the tracking algorithm in a closed-loop can be used to achieve a low residual error as calculated above.

Since we use a PC for signal processing, it is important to analyze the properties of off-the-shelf sound cards. Unfortunately, sound cards can show high sample rate offsets of up to 50 Hz at 48 kHz nominal sample rate. A sample rate offset has a similar effect on OFDM signals as the frequency offset. The only difference is that the effect depends on the sub-carrier index k. If we assume that the frequency error is zero at some index k_DC, the ICI noise caused by the sample rate offset is highest at the most distant carrier. The ICI power due to sample rate offset has been computed according to [4] and is shown in Fig. 2 for robustness mode A and the maximum possible bandwidth of 20 kHz. Here, we assume that

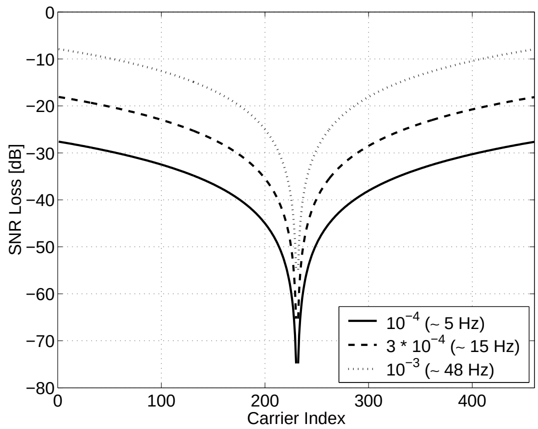

Fig. 2. SNR Loss due to sample frequency offset, relative offsets (robustness mode A with carrier spacing 41.66 Hz, 20 kHz bandwidth).

the frequency is correct in the middle of the spectrum. Unfortunately, the frequency pilots of an actual DRM signal are not located in the middle of the spectrum so that the ICI power will even be higher. If we look at the formula of ϕ_k and Fig. 1, we can conclude that for a tolerable SNR loss the total frequency error is 1 % and the relative sample rate offset ζ must be roughly $|k_\mathrm{max} - k_\mathrm{DC}|$ times lower than this frequency error. In our case ζ should be kept $< 10^{-4}$. This can be achieved by correcting the sample rate of the input signal before performing the FFT.

The resulting system structure is shown in Fig. 3.

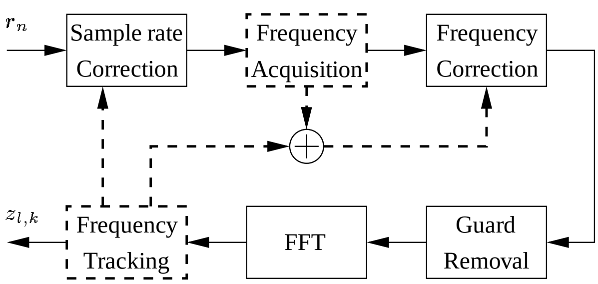

Fig. 3. Structure of the system.

III. FREQUENCY TRACKING

Although frequency acquisition precedes the tracking, it seems advantageous to analyze the tracking first to find out what residual frequency error the tracking can cope with.

Looking at Equ. 1 and assuming that the channel H_k is constant during two symbol periods T_s, we can compute the phase increment $\Delta\varphi_k = 2\pi \frac{N_\mathrm{s}}{N}\phi_k$ between two symbols:

$$\frac{\Delta\varphi_k}{2\pi T_\mathrm{s}} = \frac{\phi_k}{T_\mathrm{u}} = \Delta f + \frac{\zeta}{T_\mathrm{u}} k \qquad (3)$$

For the time being we neglect sample rate offset and concentrate on frequency offset Δf. In [6], a frequency estimator is derived which is suitable for frequency tracking in frequency selective channels:

$$\hat{\Omega}\, T_\mathrm{s} = \arg\left\{ \sum_{j=0}^{L_\mathrm{F}-1} \left(z_{l+1,p_\mathrm{f}(j)}(\hat{f}_\mathrm{acq})\, z^*_{l,p_\mathrm{f}(j)}(\hat{f}_\mathrm{acq}) \right) \right\}, \qquad (4)$$

where $\hat{\Omega} = 2\pi\,\Delta\hat{f}$ and $p_\mathrm{f}(j)$ are the positions of the frequency pilots. This estimator is utilized to track the three ($L_\mathrm{F} = 3$) frequency correction pilots in the DRM signal. The estimation is based on the phase increment given by Equ. 3. The parameter $\hat{f}_\mathrm{acq}$ shall mean that the output of the FFT unit is based on the initial frequency offset estimate done by the acquisition unit covered in the next section.

The characteristic curve of frequency tracking unit is shown in Fig. 4. We can see that the tracking works almost linear up to an offset of $\sim 25\%$ of the carrier spacing. The initial acquisition frequency must therefore fall into this range.

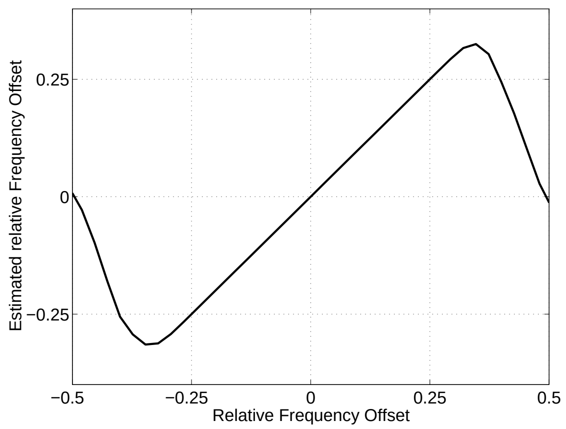

Fig. 4. Characteristic curve of frequency tracking unit.

Theoretical estimation error variances for AWGN are also given in [6]:

$$\mathrm{Var}\{\hat{\Omega}T_\mathrm{s}\} = \frac{1}{L_F}\frac{\mathrm{E}\{\,|a|^2\}}{\mathrm{E}\{\,|c|^2\}}\left(\frac{1}{\gamma} + \frac{2\,\mathrm{E}\{\,|a|^2\}}{\mathrm{E}\{\,|c|^2\}}\frac{1}{(2\gamma)^2}\right), \qquad (5)$$

where $\mathrm{E}\{\,|a|^2\}$ is the variance of the data symbols, $\mathrm{E}\{\,|c|^2\}$ is the variance of the pilots and γ is the SNR.

On frequency and time selective channels the estimate still works but the variance is higher. Depending on the Doppler spread $D_\mathrm{s} = 2f_\mathrm{d}$ of the fading the variance drops slower at higher SNR. The fast fading causes additional ICI which for Gaussian shaped Doppler spectra can be approximated as additional noise with variance [5, (3.10)]

$$\sigma^2_\mathrm{fad} \approx \frac{\pi^2}{3}(f_\mathrm{d}T_\mathrm{u})^2, \qquad (6)$$

which is twice as high as the ICI noise caused by Jakes Doppler spectrum considered in [2]. The second and more severe effect is that the channel changes considerably between two successive OFDM symbols causing additional phase noise in the phase increment given by Equ. 3.

The sample rate offset estimator uses the frequency offset estimation of each of the three frequency pilots. It calculates the difference between two pilot frequencies and relates it to the desired one. This can be written as

$$\hat{\zeta} = \frac{N}{4\pi N_\mathrm{s}} \sum_{j=1}^{2} \frac{\hat{\Omega}_j - \hat{\Omega}_0}{p_\mathrm{f}(j) - p_\mathrm{f}(0)}, \qquad (7)$$

$$\hat{\Omega}_j T_\mathrm{s} = \arg\left\{ z_{l+1,p_\mathrm{f}(j)}(\hat{f}_{acq})\, z^*_{l,p_\mathrm{f}(j)}(\hat{f}_{acq}) \right\}, \qquad (8)$$

where N is the length of the FFT and N_s is the length of one OFDM symbol. The variance of sample rate estimation is much higher than the frequency offset estimation since very small frequency differences are analyzed. This drawback can be compensated by averaging a lot of estimations which, of course, may take a long time. But since the sample rate offset is only caused by the A/D-converter local oscillator which is usually very stable, tracking time is not critical and sample rate offset estimation results can even be saved and reused the next time the receiver is started.

IV. FREQUENCY ACQUISITION

Several frequency acquisition algorithms have been published. Unfortunately, they all have drawbacks which prevented their utilization in our receiver. The acquisition in [6] proposes to use Equ. 4 with trial frequencies and than search for the maximum. This would lead to unacceptably long acquisition times as the search space is several times the carrier spacing and therefore too large. Algorithms that employ a guard interval correlation [7] suffer from the severe ISI that is expected for DRM. Thus we looked for alternatives.

The proposed frequency acquisition algorithm explores the power difference between pilot cells and data cells. On the frequency pilot carriers there are only cells with boosted power whereas on the other carriers data cells with low power alternate with boosted gain pilots (in the worst case of robustness mode C, the ratio is $1/1$). Furthermore, we make use of differences in power spectral density of frequency pilots and data cells. The frequency pilots are discrete lines in the frequency domain if the channel is static. The power spectral density of the data cells is $\sim \mathrm{sinc}^2$ [8] which causes a spreading of their power. If we estimate the power spectral density with a fine frequency resolution and use a lot of symbols for averaging, the discrete spectral lines of the three frequency pilots will clearly show up in the spectrum.

The basic idea of our acquisition algorithm is to calculate an FFT over more than one symbol and correlate the squared norm of this result with the known frequency pilot positions. Since this FFT operation is just an estimation of the power spectral density, the placement of the FFT window is arbitrary. This is an advantage of this algorithm since no prior timing information is needed. The range of the correlation determines the search window of the acquisition. This can be as small as the maximum frequency error of the analog down-converter part of the receiver. Assuming this error is 100 ppm which is equivalent to a maximum error of ± 3 kHz at the upper end of the shortwave band at 30 MHz, we get an interval of 6 kHz. The preliminary estimate of the estimated frequency offset at the time index l is calculated as

$$\hat{f}_{\mathrm{acq}}(l) = \frac{f_{\mathrm{s}}}{N_{\mathrm{ac}}} \max_{m} \left\{ \sum_{i=0}^{2} R_{m+p_{\mathrm{fac}}(i),l} \right\}, \qquad (9)$$

$$R_{m,l} = \left| \sum_{n=0}^{N_{\mathrm{ac}}-1} r_{n+l}\, e^{-j\frac{2\pi}{N_{\mathrm{ac}}}nm} \right|^2, \qquad (10)$$

where f_{s} is the sampling frequency, $p_{\mathrm{fac}}(i)$ are the modified positions of the frequency pilots and N_{ac} is the number of received samples r_n over which the FFT is calculated. The maximum search is performed over these indices m which are in the search window of the acquisition (± 3 kHz from the DC-frequency).

The parameter N_{ac} should be chosen so that the frequency pilots are covered by the resulting grid in the frequency domain. This can be assured by setting it to a multiple of the total symbol length. In that case the modified positions $p_{\mathrm{fac}}(i)$ are calculated as follows:

$$p_{\mathrm{fac}}(i) = p_{\mathrm{f}}(i) N_{\mathrm{sym}} \left(\frac{T_{\mathrm{g}}}{T_{\mathrm{u}}} + 1 \right), \quad i = 0, 1, 2 \quad (11)$$

where $p_{\mathrm{f}}(i)$ are the carrier indices tabulated in [1], T_{g} and T_{u} are the durations of guard interval and useful part and N_{sym} is the number of symbols we want to use for averaging.

The larger N_{sym} is chosen, the more distinct the statistical properties are and the better the peaks can be detected. But on the other hand if the number N_{sym} is getting larger, channel effects reduce the performance (especially on fast fading channels). To get a good trade-off between these effects, we set $N_{\mathrm{sym}} = 4$. That gives us a frequency resolution of $<25\,\%$ of the carrier spacing which is sufficient for the tracking unit. But using this small amount of symbols can lead to unwanted peaks in the data carriers due to the poor averaging which results in false acquisition frequency estimations. If additionally one or more frequency pilots are attenuated by the channel transfer function, this effect is increased. However, to improve the statistics, we use Equ. 9 to calculate three preliminary estimates at successive symbols (that means $l = 0, N_{\mathrm{s}}, 2N_{\mathrm{s}}$, where N_{s} is the number of samples per symbol). These estimates are compared and if they are equal, the final acquisition frequency estimation is found. If they are not equal, a set of three new estimates shifted by one symbol is calculated (which means $l = N_{\mathrm{s}}, 2N_{\mathrm{s}}, 3N_{\mathrm{s}}$). This is repeated until all three estimates are equal.

Extensive simulations have shown that the average number of trials is approximately 4 which makes a total acquisition delay of 6 symbols. The average error rate of this algorithm is smaller than 10% for all channels even at very low SNRs.

V. SIMULATION

All simulations were performed on a DRM teststream which includes all pilot cells defined in [1] and a random 64-QAM modulation on the data cells. Actually, data cells can have different modulations (4-, 16- or 64-QAM) but since they are normalized, the effect on the frequency synchronization algorithms can be neglected. The channels 1-6 are WSSUS with the profiles defined in [1].

In Fig. 5, the theoretically derived error estimation of the frequency tracking unit (Equ. 5) is compared to a simulation using all four robustness modes. The

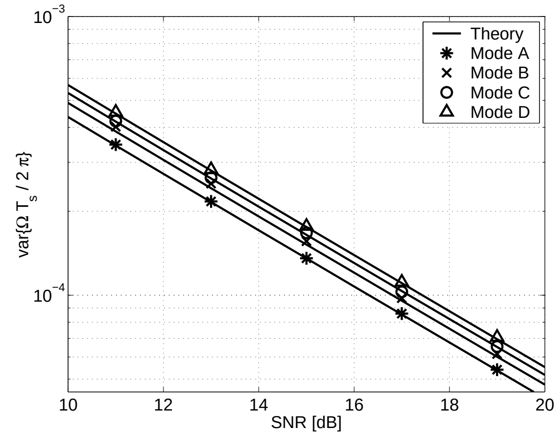

Fig. 5. Tracking variance, AWGN channel, robustness modes A-D.

scattered pilots and the boosted pilots of the DRM signal contribute to the variance of a. This explains the slightly different variance of the four robustness modes as they differ in the amount of pilots and thus in $\mathrm{E}\{|a|^2\}$. The simulation results are in very good agreement with the analytically derived formula despite the fact that only three pilots are used.

Fig. 6 shows simulation results of the tracking variance using all channels. Especially the fast fading channels 5 and 6 cause strong performance degradation at high SNRs which result from the impact of the time selectivity. But still good performance of the estimator can be expected in a closed loop as the variance of the estimator is very low even for the fast fading channels.

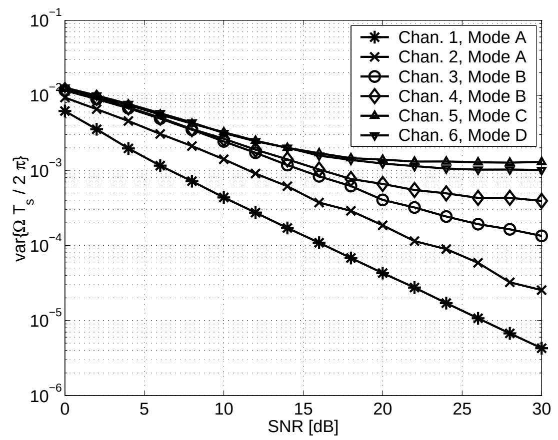

Fig. 6. Simulated tracking variance for all channels.

VI. Conclusion

In this paper we proposed a frequency synchronization strategy which is sufficient for DRM signals. A two stage frequency synchronization consisting of acquisition and tracking was presented and analyzed. It was shown that sample rate offset correction is necessary for a PC-based receiver since sample rate offsets can have severe influence on the performance of the receiver. Both tracking and acquisition was analyzed by simulation. It was found that the acquisition, despite its simplicity, yields an initial frequency estimate that is sufficient for the tracking algorithm. The probability of false detection was $<10\,\%$ which is acceptable for a broadcast receiver. The tracking showed low variances of the estimate and could also be used to track the sample rate offset. The presented algorithms are part of our PC-based DRM receiver implementation and perform very well in practice.

References

[1] European Telecommunications Standards Institute: Digital Radio Mondiale (DRM), *System Specification ETSI TS 101980*, 2001.

[2] M. Speth and H. Meyr: Optimum Receiver Design for Wireless Broad-Band Systems Using OFDM – Part I. *IEEE Trans. Commun.*, Vol. COM-47(11), 1668–1677, 1999

[3] M. Speth and H. Meyr: Optimum Receiver Design for OFDM-Based Broadband Transmission – Part II: A Case Study. *IEEE Trans. Commun.*, Vol. COM-49(4), 571–578, 2001

[4] B. Stanchev and G. Fettweis: Time-Variant Distortions in OFDM. *IEEE Commun. Letters*, Vol. 4(4), 312–314, 2000

[5] Y. Li and L. Cimini Jr.: Bounds on the Interchannel Interference of OFDM in Time-Varying Impairments. *IEEE Trans. Commun.*, Vol. COM-49(3), 401–404, 2001

[6] F. Claßen and H. Meyr: Synchronization Algorithms for an OFDM System for Mobile Communication. *1. ITG Fachtagung Codierung für Quelle, Kanal und Übertragung*, ITG Fachbericht 130, 105–113, 1994

[7] J. van de Beek, M. Sandell, P. Borjesson: ML Estimation of Time and Frequency Offset in OFDM Systems. *IEEE Trans. Signal Processing*, Vol. 45(7), 1800-1805, 1997

[8] J. G. Proakis: Digital Communications McGraw-Hill, 1995